ADVANCES IN ATMOSPHERIC SCIENCES, VOL. 26, NO. 3, 2009, 577–584

Parameterizations of the Daytime Friction Velocity, Temperature Scale, and Upslope Flow over Gently Inclined Terrain in Calm Synoptic Conditions

ZHANG Zhanhai[1,2] (张占海), ZHOU Mingyu*[1,2] (周明煜), Sharon ZHONG[3], Donald H. LENSCHOW[4], and Qing WANG[5]

[1] *Key Laboratory for Polar Science, Polar Research Institute of China, Shanghai* 200136

[2] *State Key Laboratory of Atmospheric Boundary Layer Physics and Atmospheric Chemistry, Institute of Atmospheric Physics, Chinese Academy of Sciences, Beijing* 100029

[3] *Department of Geography, Michigan State University, East Lansing, MI* 48824-111*, USA*

[4] *National Center for Atmospheric Research, Boulder, CO* 80307*, USA*

[5] *Department of Meteorology, Naval Postgraduate School, Monterey, CA* 93943*, USA*

(Received 22 July 2008; revised 19 November 2008)

ABSTRACT

A set of new parameterizations for the friction velocity and temperature scale over gently sloped terrain and in calm synoptic conditions are theoretically derived. The friction velocity is found to be proportional to the product of the square root of the total accumulated heating in the boundary layer and the sinusoidal function of the slope angle, while the temperature scale is proportional to the product of the boundary layer depth, the sinusoidal function of the slope angle and the potential temperature gradient in the free atmosphere. Using the new friction velocity parameterization, together with a parameterization of eddy diffusivity and an initial potential temperature profile around sunrise, an improved parameterization for the thermally induced upslope flow profile is derived by solving the Prandtl equations. The upslope flow profile is found to be simply proportional to the friction velocity.

Key words: friction velocity, temperature scale, slope terrain, flux-profile relationship, upslope flow

Citation: Zhang, Z. H., M. Y. Zhou, S. Zhong, D. H. Lenschow, and Q. Wang, 2009: Parameterizations of the daytime friction velocity, temperature scale, and upslope flow over gently inclined terrain in calm synoptic conditions. *Adv. Atmos. Sci.*, **26**(3), 577–584, doi: 10.1007/s00376-009-0577-z.

1. Introduction

In fair weather conditions, thermally induced up-valley and up-slope flows prevail over complex terrain during the daytime. These terrain-induced flows may interact with the regional and synoptic-scale flows to trigger convective precipitation, modify the wind direction in the planetary boundary layer (PBL), and affect the surface-atmosphere exchange of momentum, heat and water vapor. It is, therefore, important to properly account for their effect in weather forecasting and climate models. Many previous studies have used observations (Whiteman, 1982; Stewart et al., 2001; Hunt et al., 2003), laboratory experiments (Chen et al., 1996; Hunt et al., 2003) and numerical simulations (e.g., McNider and Pielke, 1981; Pielke, 1984; Pielke and Segal, 1986; Abbs and Pielke, 1986; Stephan et al., 2002; Zhong et al., 2004) to examine the characteristics of the upslope flows (u) and the surface fluxes of momentum and sensible heat ($\overline{w'u'_0}$ and $\overline{w'\theta'_0}$). It is evident from these studies that the strength of the thermally forced slope flows and the surface fluxes of momentum and heat are closely related to the slope angle (α) and the amount of accumulated heating in

*Corresponding author: ZHOU Mingyu, mingyuzhou@yahoo.com

the PBL after sunrise defined by

$$Q = \int_{z_0}^{h+z_0} [\theta(z) - \theta_0(z)]dz \,, \tag{1}$$

where $\theta(z)$ and $\theta_0(z)$ are the potential temperatures over a given slope site at t and $t = 0$ (around sunrise), respectively; z, the vertical coordinate with $z = 0$ at the slope surface; z_0, the surface roughness; and h, the PBL depth. The accumulated heating rate Q is related to the surface sensible heat flux and slope angle through the following relationship

$$\begin{aligned} Q &= \int_{z_0}^{h+z_0} [\theta(z) - \theta_0(z)]dz \\ &= \int_0^t \left[(1+\delta_h)\overline{w'\theta'_0} + \int_{z_0}^{h+z_0} \beta_{\rm T} u \sin\alpha dz \right] dt \,, \end{aligned}$$

where $\beta_{\rm T}$ is the vertical gradient of $\theta(z)$ in the free atmosphere and δ_h is the entrainment rate for the sensible heat flux (under synoptically calm conditions, a zero-order jump model in the daytime PBL is used in the current study for simplification). We define θ'' as

$$\theta''(z) \equiv \theta(z) - \theta_0(z) \,. \tag{2}$$

Despite the known fact that these variables, $u(z)$, $\overline{w'u'_0}, \overline{w'\theta'_0}, Q$, and α, are closely related to each other, few quantitative relationships among them have been derived. Such relationships may be obtained theoretically by integrating the classical Prandtl equations for $u(z)$ and $\theta(z)$:

$$\frac{\partial u}{\partial t} = \lambda\theta'' \sin\alpha + \frac{\partial \overline{w'u'}}{\partial z} \,, \tag{3}$$

$$\frac{\partial \theta}{\partial t} = -\beta_{\rm T} u \sin\alpha + \frac{\partial \overline{w'\theta'}}{\partial z} \,, \tag{4}$$

where $\lambda = g/\theta_0$ is a buoyancy parameter. $\overline{w'u'}$ and $\overline{w'\theta'}$ are the turbulent fluxes of momentum and sensible heat, which can be estimated using the gradient of the mean wind and potential temperature $\overline{w'u'} = K_{\rm m}(z)\partial u(z)/\partial z$ and $\overline{w'\theta'} = K_{\rm T}(z)(\partial\theta(z)/\partial z - \gamma_{\rm cg})$ with $\gamma_{\rm cg}$ being a temperature counter-gradient and $K_{\rm m}$ and $K_{\rm T}$, the eddy diffusivities for momentum and heat. Assuming that the upslope flow along the middle of a long homogeneous gentle slope does not vary and that $\gamma_{\rm cg} = 0$ and $K_{\rm m}(z) = K_{\rm T}(z) = K(z)$ =constant, Defant (1951) provided a classical schematic illustration of the diurnal cycle of a thermally forced circulation through an infinitely deep atmosphere. For steady-state, the upslope flow depth and the maximum wind speed ($u_{\rm max}$) from the Defant (1951) solution can be expressed as:

$$h = \pi \left(\frac{2K}{N \sin\alpha} \right)^{1/2} \,, \tag{5}$$

$$u_{\rm max} = \frac{\lambda\Delta\theta}{\sqrt{2}N} e^{-\frac{\pi}{4}} \,, \tag{6}$$

where $N = (\lambda\beta_{\rm T})^{1/2}$ is the Brunt-Väisälä frequency and $\Delta\theta$ is the value of $\theta''(z)$ at the slope surface. The upslope flow depth is assumed to be the same as the PBL depth. Equations (5) and (6) indicate that the depth of the upslope flow layer decreases as the slope angle increases, while the maximum slope flow speed is independent of the slope angle.

The surface turbulent fluxes are typically computed based on either the surface layer similarity or a bulk parameterization (Chou et al., 2003; Bourras, 2006; Princevac and Venkatram, 2007; Venkatram and Princevac, 2008). There has been some theoretical work with respect to the parameterization of the turbulent characteristics over slopping terrain. Gutman and Melgarejo (1981) derived an analytical expression for the friction velocity u_{*0}, and the temperature scale θ_{*0}, as functions of $\beta_{\rm T}$ and α over a slightly inclined terrain. Hunt et al. (2003) proposed that u_{*0} is proportional to $w_*\alpha^{1/3}$ for a gentle slope, where w_* is the convective velocity.

The present study attempts to examine how the slope angle (α) and the accumulated heating rate in the PBL (Q) affect the friction velocity u_{*0}, the temperature scale θ_{*0}, and the thermally induced upslope flow profile $u(z)$. This is achieved through derivations of the theoretical relationships based on the Prandtl equations and under synoptically calm and steady conditions in a meso-β domain.

2. Formula for the friction velocity

Assume near calm synoptic conditions and steady state, substituting $\overline{w'u'} = u_*^2$ into Eq. (3) yields:

$$\frac{\partial u_*^2(z)}{\partial z} = -\lambda\theta''(z)\sin\alpha \,. \tag{7}$$

Integrating Eq. (7) with respect to z from $z = z_0$ to $z = z_0 + h$, for the boundary conditions: $u_*^2(z) = u_{*0}^2$ at $z = z_0$ and $u_*^2(z) = -\delta_{\rm m} u_{*0}^2$ at $z = z_0 + h$, we obtain

$$u_{*0}^2 = \frac{\lambda Q \sin\alpha}{1+\delta_{\rm m}} \,, \tag{8}$$

$$u_{*0} = \left(\frac{\lambda Q \sin\alpha}{1+\delta_{\rm m}} \right)^{1/2} \,, \tag{9}$$

where $\delta_{\rm m}$ is the entrainment rate for momentum.

Equation (9) shows that in calm synoptic conditions over sloping terrain, u_{*0} depends on both thermodynamic (Q) and dynamic (α) processes and that the u_{*0} is proportional to $(Q\sin\alpha)^{1/2}$ and independent of the vertical distribution of $\theta''(z)$. Notice that α is considered a dynamic factor because of the clear linkage between the strength of the thermally forced upslope flow and u_{*0}: both are proportional to $(\sin\alpha)^{1/2}$ as described by Eq. (9) above and Eq. (20) below.

As will be shown next, this new parameterization for u_{*0} is very important in deriving a theoretical formula for the upslope wind profile $u(z)$.

3. Formula for thermally-forced upslope flows

A theoretical formula for the upslope wind profile $u(z)$ as a function of the PBL heating rate Q and slope angle α, can be derived by integrating Eq. (3) if the turbulent momentum flux $\overline{w'u'}$ and the perturbation potential temperature θ'' are known. In sections 3.1 and 3.2, we describe how $\overline{w'u'}$ and θ'' are parameterized using the new parameterization for u_{*0} and typical profiles for potential temperature.

3.1 *Model for the turbulent eddy diffusivity*

As described earlier, as a first order approximation, the turbulent momentum flux in $\overline{w'u'}$ in Eq. (3) can be parameterized using $\overline{w'u'} = K_{\rm m}(z)\partial u(z)/\partial z$ where $K_{\rm m}$ is the eddy diffusivities for momentum and $\partial u(z)/\partial z$ is the vertical wind shear.

The simplest approach is to assume that $K(z)$ is a constant (e.g., Kao, 1981; Ye et al., 1987). A somewhat more sophisticated formula for $K(z)$ was proposed by Gutman and Melgarejo (1981); $K(z) = ku_{*0}z$ when $z \leqslant -0.07L$, and $K(z) \sim (\overline{w'\theta'_0})^{1/3}z^{4/3}$ when $z \geqslant -0.07L$ (k is the von Karman constant and L is the Obukhov length). Stevens (2000) presented an analytic solution to a PBL model with a cubic eddy diffusivity profile for the potential temperature. O'Brien (1970) obtained a cubic polynomial formulation for $K(\xi)$ in the PBL where $\xi = z/h$ is a non-dimensional height. This formulation has been used extensively in numerical models (Pielke et al., 1983; Troen and Mahrt, 1986), but rarely in analytical studies, possibly because of its complexity.

In order to derive a reasonable vertical profile of $u(z)$, a cubic $K_{\rm m}$ profile, as described by O'Brien (1970), Pielke et al. (1983); Troen and Mahrt (1986), (see Appendix B of Ye et al., 1987) is used in this study:

$$K_{\rm m}(\xi) = ku_{*0}h\xi(1+b_1-\xi)^2\,, \tag{10}$$

where $\xi = z/h$. Equation (10) indicates that $K_m(\xi)$ depends on dynamic and thermal dynamic processes through the variables u_{*0} and h [as expressed by Eq. (18)]. A small value of b_1 (b_1=0.05) is used so that the value of $K_{\rm m}(\xi)$ at the top of the PBL is slightly larger than zero, but much smaller than $K_{\rm max}$, the maximum value of $K_{\rm m}(\xi)$, which from Eq. (10), occurs at $\xi = (1+b_1)/3$.

3.2 *The determination of* $\theta''(z)$

The observational data from Wangara (Clark et al., 1971), O'Neill (Lettau and Davidson, 1957), Vampa Valley in western Colorado (Whiteman, 1982) and South Park in the Colorado Rockies (Banta and Cotton, 1981) showed that during a calm, clear day over different topography (plain, a deep mountain valley or a broad, flat basin), a representative profile of $\theta(z)$ in the daytime PBL typically consists of two layers: a shallow super-adiabatic surface layer (with a depth $h_{\rm S}$) where the potential temperature decreases rapidly with height, and a near neutral layer where the potential temperature profile is almost independent of height. The two layer structure is schematically illustrated by the thin solid line in Fig. 1. Mathematically it can be expressed as follows:

$$\theta(z) = \begin{cases} \theta(h) + \dfrac{\theta_{*0}}{k}\left[\ln\left(\dfrac{h_{\rm S}+z_0}{z}\right) + 2\ln\left(\dfrac{1+Y}{1+Y_{\rm S}}\right)\right]\,, & z_0 < z \leqslant h_{\rm S}+z_0\,, \\ \theta(h)\,, & h_{\rm S}+z_0 < z < h+z_0\,, \end{cases} \tag{11}$$

where $Y = (1-15z/L)^{1/2}$ and $Y_{\rm S} = (1-15z_0/L)^{1/2}$. A representative profile of $\theta(z)$ around sunrise [defined as $\theta_0(z)$] may consist of three layers [as schematically illustrated by the thick solid line in Fig. (1)]: a nocturnal surface inversion layer of depth h_1 that was formed the previous night; a less stable and nearly neutral layer of thickness (h_2-h_1) remaining from the previous PBL; and a nearly uniform stable layer above h_2+z_0. Mathematically, the three-layer approximation of the near sunrise potential temperature profile can be expressed as:

$$\theta_0(z) = \begin{cases} \theta_0(h_1) - \Delta\theta_1\left(1-\dfrac{z-z_0}{h_1}\right)^{n_0}\,, & z < h_1+z_0\,, \\ \theta_0(h_1)\,, & h_1+z_0 \leqslant z \leqslant h_2+z_0\,, \\ \theta_0(h_1)+\beta_{\rm T}(z-h_2)\,, & h_2+z_0 < z\,, \end{cases} \tag{12}$$

where $\theta_0(h_1)$ is the value of $\theta_0(z)$ at $z = h_1 + z_0$ and $\Delta\theta_1 = \theta_0(h_1 + z_0) - \theta_0(z_0)$ is the intensity of the surface inversion layer. An analysis of the observational data indicates that n_0 depends on the relative contributions of radiative and turbulent cooling across h_1 as discussed by André and Mahrt (1982), Yasuda et al. (1986) and Garrat and Ryan (1989). It is assumed that Eqs. (11 and 12) can be used to describe the vertical profiles of $\theta(z)$ and $\theta_0(z)$ over a given slope site.

A representative profile of $\theta''(z)$ can be derived by substituting Eqs. (11) and (12) into Eq. (2), which yields:

$$\theta''(z) = \begin{cases} \Delta\theta_1 \left(1 - \dfrac{z - z_0}{h_1}\right)^{n_0} + \beta_{\mathrm{T}}(h - h_2) + \dfrac{\theta_{*0}}{k}\left[\ln\left(\dfrac{h_{\mathrm{S}} + z_0}{z}\right) + 2\ln\left(\dfrac{1+Y}{1+Y_{\mathrm{S}}}\right)\right], & z_0 < z \leqslant h_{\mathrm{S}} + z_0\,, \\ \Delta\theta_1 \left(1 - \dfrac{z - z_0}{h_1}\right)^{n_0} + \beta_{\mathrm{T}}(h - h_2)\,, & h_{\mathrm{S}} + z_0 < z < h_1 + z_0\,, \\ \beta_{\mathrm{T}}(h - h_2)\,, & h_1 + z_0 \leqslant z \leqslant h_2 + z_0\,, \\ \beta_{\mathrm{T}}(z - h_2)\,, & h_2 + z_0 < z\,. \end{cases} \tag{13}$$

Substituting Eq. (13) into Eq. (1) and integrating Eq. (1), yields the following formula:

$$Q = Q_1 + Q_2 + Q_{\mathrm{S}}\,, \tag{14}$$

where Q_1, Q_2, and Q_{S} are defined as:

$$\begin{aligned} Q_1 &= \int_{z_0}^{h_1+z_0} \Delta\theta_1 \left(1 - \frac{z - z_0}{h_1}\right)^{n_0} dz \\ &= h_1 \Delta\theta_1/(1 + n_0)\,, \end{aligned} \tag{15}$$

$$\begin{aligned} Q_2 &= \int_{z_0}^{h_2+z_0} \beta_{\mathrm{T}}(h - h_2)dz + \int_{h_2+z_0}^{h+z_0} \beta_{\mathrm{T}}(z - h_2)dz \\ &= \beta_{\mathrm{T}}(h^2 - h_2^2)/2\,, \end{aligned} \tag{16}$$

$$\begin{aligned} Q_{\mathrm{S}} &= \int_{z_0}^{z_0+h_{\mathrm{S}}} \frac{\theta_{*0}}{k}\left[\ln\left(\frac{h_{\mathrm{S}}+z_0}{z}\right) + 2\ln\left(\frac{1+Y}{1+Y_{\mathrm{S}}}\right)\right] dz \\ &= \frac{\theta_{*0}}{k}\left\{z_0\left[\ln\left(\frac{z_0+h_{\mathrm{S}}(x)}{z_0}\right) + 2\ln\left(\frac{1+Y_0}{1+Y_{\mathrm{S}}}\right)\right] + \right. \\ &\quad \left. \frac{2L}{15}(Y_{\mathrm{S}} - Y_0)\right\}\,. \end{aligned} \tag{17}$$

Q_1 represents the integrated nocturnal cooling across h_1 formed the previous night and Q_{S} is the integrated heating across the daytime super-adiabatic layer.

For commonly observed daytime upslope flows, the steady-state values of Q and Q_{S} are in order of 10^3 (K m s^{-1}) and 10^1 (K m s^{-1}), respectively, yielding a ratio of Q_{S}/Q of 10^{-2}. Q_{S} can thus be eliminated from Eq. (14), suggesting that it is not necessary to include the super-adiabatic surface layer in the solution for Eqs. (14) and (16). This leads to the following approximation for h:

$$h \cong \left[h_2^2 + \frac{2(Q - Q_1)}{\beta_{\mathrm{T}}}\right]^{1/2}\,, \tag{18}$$

Equation (13) can now be simplified to

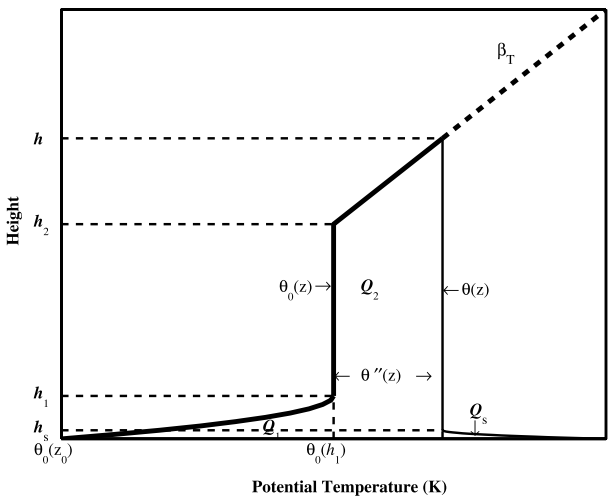

Fig. 1. Schematic illustration of the $\theta_0(z)$ profile (thick solid line) and $\theta(z)$ profile (thin solid line); h_{S}, h_1, h_2 and h on the vertical axis are the super-adiabatic surface layer depth, the nocturnal inversion layer depth formed during the previous night, the top of the nearly neutral layer remaining from the previous day's PBL and the daytime PBL depth, respectively; Q_1, the total cooling across h_1; Q_{S}, the heating relative to the daytime super-adiabatic surface layer; and $Q_2 = Q - Q_1 - Q_{\mathrm{S}}$.

$$\theta''(\xi) = \begin{cases} \Delta\theta_1 \left(1 - \dfrac{\xi - \xi_0}{\xi_1}\right)^{n_0} + \beta_{\mathrm{T}} h(1-\xi_2)\,, & \xi_0 < \xi < \xi_1 + \xi_0\,, \\ \beta_{\mathrm{T}} h(1-\xi_2)\,, & \xi_1 + \xi_0 \leqslant \xi \leqslant \xi_2 + \xi_0\,, \\ \beta_{\mathrm{T}} h(\xi - \xi_2)\,, & \xi_2 + \xi_0 < \xi \leqslant 1 + \xi_0\,, \end{cases} \tag{19}$$

where $\xi_0 = z_0/h$, $\xi_1 = h_1/h$ and $\xi_2 = h_2/h$.

3.3 *Analytical results and discussions*

Equation (19) indicates that the value of $\theta''(z)$ increases with decreasing z. Eq. (7) together with Eq. (19) suggests that $\partial u_*^2/\partial z$ near the surface is larger than that in the rest of the PBL. In other words, the value of $u_*^2(z)$ near the surface deviates more from the constant flux than in the overlying layer. Therefore, a constant momentum layer is not considered in the current derivation.

Under synoptically stagnant conditions and in steady-state, the thermally forced upslope flow profile, $u(\xi)$, can be derived by substituting $\overline{w'u'} = K_{\mathrm{m}}(z)\partial u(z)/\partial z$ into Eq. (3), Eq. (9) into Eq. (10), and then Eqs. (10) and (19) into Eq. (3), and integrating the resulting equation with respect to ξ, using boundary conditions $u(\xi) = 0$ at $\xi = \xi_0$ and at $\xi = 1 + \xi_0$ and the conjugation conditions of $u(z)$ and $\partial u(z)/\partial z$ at $\xi = \xi_1 + \xi_0$ and at $\xi = \xi_2 + \xi_0$. The result of the integration is

$$u(\xi) = \left[\frac{(1+\delta_{\mathrm{m}})Q\lambda\sin\alpha}{k}\right]^{1/2} f(\xi)\,, \tag{20}$$

Substituting Eq. (9) to Eq. (20) yields

$$u(\xi) = \frac{(1+\delta_{\mathrm{m}})}{k^{1/2}} u_{*0} f(\xi)\,, \tag{21}$$

$$f(\xi) = \begin{cases} f_1(\xi)\,, & \xi_0 < \xi < \xi_1 + \xi_0\,, \\ f_2(\xi)\,, & \xi_1 + \xi_0 \leqslant \xi \leqslant \xi_2 + \xi_0\,, \\ f_3(\xi)\,, & \xi_2 + \xi_0 < \xi \leqslant 1 + \xi_0\,, \end{cases} \tag{22}$$

where

$$f_1(\xi) = \frac{Q_1}{Q}[A_2(\xi) - A_2(\xi_0)] + \frac{2Q_2/Q}{1+\xi_2}[B_1(\xi_0) - B_1(\xi)] - C_{11}[B_3(\xi) - B_3(\xi_0)]\,, \tag{23}$$

$$f_2(\xi) = \frac{Q_1}{Q}[A_2(\xi_1 + \xi_0) - A_2(\xi_0)] + \frac{2Q_2/Q}{1+\xi_2}[B_1(\xi_0) - B_1(\xi)] - C_{11}[B_3(\xi) - B_3(\xi_0)]\,, \tag{24}$$

$$\begin{aligned} f_3(\xi) =& \frac{Q_1}{Q}[A_2(\xi + \xi_0) - A_2(\xi_0)] + \\ & \frac{2Q_2/Q}{1+\xi_2}[B_1(\xi_0) - B_1(\xi_2 + \xi_0)] - \\ & C_{11}[B_3(\xi) - B_3(\xi_0)] + \\ & \frac{Q_2/Q}{(1-\xi_2^2)}\{(1 + 2\xi_0 - b_1)[B_1(\xi_2 + \xi_0) - B_1(\xi)] + \\ & \ln\frac{1 + b_1 - \xi}{1 + b_1 - \xi_2 - \xi_0} - \\ & \frac{(\xi_2 + \xi_0)^2}{1 + b_1}[B_3(\xi_2 + \xi_0) - B_3(\xi)]\} \end{aligned} \tag{25}$$

with A_2, B_1, B_2, and B_3 defined as

$$\begin{aligned} A_2(\xi) =& \int \frac{\left(1 - \dfrac{\xi - \xi_0}{\xi_1}\right)^{n_0}}{\xi(1 + b_1 - \xi)^2} d\xi \\ =& \frac{e_0}{(1+b_1)} B_3(\xi) + \frac{e_1}{(1+b_1)} B_2(\xi) + \\ & \sum_{j=2}^{1+n_0} e_j[(1+b_1)^{j-2}\ln\xi + \\ & \sum_{i=1}^{j-2} C_{j-2}^i (1+b_1)^{j-2-i}(-\xi)^i/i]\,, \end{aligned} \tag{26}$$

$$B_1(\xi) = 1/(1 + b_1 - \xi)\,, \tag{27}$$

$$B_2(\xi) = \ln[\xi/(1 + b_1 - \xi)]\,, \tag{28}$$

$$B_3(\xi) = \frac{B_2(\xi)}{(1+b_1)} + B_1(\xi)\,, \tag{29}$$

$$e_j = \frac{C^j_{1+n_0}}{\xi_1^j}\left(1-\frac{1+b_1-\xi_0}{\xi_1}\right)^{1+n_0-j}, \quad j=0,1,2,\ldots \tag{30}$$

$$C^j_{1+n_0} = \frac{j!}{(1+n_0-j)!j!}, \tag{31}$$

$$C^i_{j-2} = \frac{i!}{(j-2-i)!i!}, \tag{32}$$

and

$$C_{11} = \frac{\text{term1}}{\text{term2}}, \tag{33}$$

$$\begin{aligned}\text{term1} =& \frac{Q_1}{Q}[A_2(\xi_1+\xi_0)-A_2(\xi_0)]+\\ & \frac{Q_2/Q}{(1-\xi_2^2)}\{\ln\frac{1+b_1-\xi_2-\xi_0}{b_1-\xi_0}+\\ & (1+2\xi_0-b_1)[B_1(1+\xi_0)-B_1(\xi_2+\xi_0)]-\\ & \frac{(\xi_2+\xi_0)^2}{1+b_1}[B_3(1+\xi_0)-B_3(\xi_2+\xi_0)]\}-\\ & \frac{2Q_2/Q}{(1+\xi_2)}[B_1(\xi_0)-B_1(\xi_2+\xi_0)]\end{aligned}$$

and term2$=B_3(\xi_0)-B_3(1+\xi_0)$.

If φ is used to denote A_2, B_1, B_2, or B_3, then $\varphi(\xi_0), \varphi(\xi_2+\xi_0)$, and $\varphi(1+\xi_0)$ are the values of $\varphi(\xi)$ at $\xi=\xi_0, \xi=\xi_2+\xi_0$, and $\xi=1+\xi_0$, respectively.

Note that $f(\xi)$ is independent of the slope steepness and that from Eq. (20), $u(\xi)$ is proportional to $\sqrt{\sin\alpha}$. These results are consistent with results from previous numerical simulations. For example, Ye et al. (1987) based on idealized numerical simulations concluded, that over a plain-slope-plateau topography the maximum upslope flow intensity over the middle of the slope in mid afternoon is proportional to $\sqrt{\sin\alpha}$.

Equation (22) shows that $f(\xi)$ is a complicated function of $Q_1/Q, Q_2/Q, h_1, h_2$, and h; the impact of Q on $f(\xi)$ is unclear based on Eqs. (26)–(33). The impact of Q on $f(\xi)$ can be assessed through a case computation using Eq. (22), which is shown in Fig. 2. The dotted and solid lines in Fig. 2, which correspond to Q=1155 m K and 3135 m K, were computed with β_T=4.0 K km^{-1}, z_0=0.04 m, n_0=1, Q_1=330 m K, h_1=150 m and h_2=1000 m. When Q increases from 1155 m K to 3135 m K (by 170%), the profiles of $f(\xi)$ are almost the same in the layer near the surface and near h. In the middle area, the impact of the variation of Q on $f(\xi)$ is very small. The maximum value of $f(\xi), f_{\max}$, increases from 5.27 to 5.70 (increasing only 8%). Additional computation also indicates that

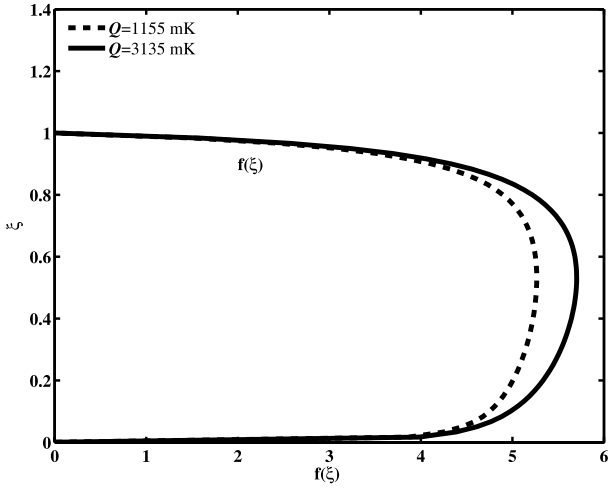

Fig. 2. The $f(\xi)$ profiles for Q=1155 m K (dotted lines) and 3135 m K (solid lines) computed based on Eqs. (22)–(33) with β_T=4.0 K km^{-1}, z_0=0.04 m, n_0=1, Q_1=330 m K, h_1=150 m, and h_2=1000 m.

when Q increases from 990 m K to 3795 m K (an increase of 283%), the value of $f_{\max}$ increases from 5.17 to 5.76 (an 11% increase). Therefore, we conclude that as a first-order approximation, the impact of Q on $f(\xi)$ can be neglected, which, according to Eq. (20), suggests that $u(\xi)$ is proportional to $Q^{1/2}$.

According to the above analysis, $u(\xi)$ is proportional to $(Q\sin\alpha)^{1/2}$; the proportional coefficient, $f(\xi)$, as illustrated in Fig. 2, is independent of α and nearly independent of Q.

4. Formula for the temperature scale

A new parameterization for θ_{*0} over slopping terrain in a synoptically calm condition is derived as follows:

Substituting $\overline{w'\theta'} = u_*\theta_*(z)$ into Eq. (4) under steady-state conditions results in:

$$\frac{\partial u_*\theta_*(z)}{h\partial\xi} = \beta_T u(z)\sin\alpha\,. \tag{34}$$

Integrating Eq. (34) with respect to ξ from $\xi=\xi_0$ to $\xi=1+\xi_0$, for the given boundary conditions: $u_*\theta_*(\xi)=u_{*0}\theta_{*0}$ at $\xi=\xi_0$ and $u_*\theta_{*0}(\xi)=-\delta_h u_{*0}\theta_{*0}$ at $\xi=1+\xi_0$ yields

$$u_{*0}\theta_{*0} = -\frac{\beta_T h\sin\alpha}{1+\delta_h}\int_{\xi_0}^{1+\xi_0} u(\xi)d\xi\,. \tag{35}$$

Substituting Eq. (21) into Eq. (35) yields

$$\theta_{*0} = -\beta_T h\sin\alpha\frac{(1+\delta_m)}{k^{1/2}(1+\delta_h)}\eta(\xi)\,, \tag{36}$$

$$\eta(\xi) = \int_{\xi_0}^{1+\xi_0} f(\xi) d\xi \,. \tag{37}$$

As mentioned above, $f(\xi)$ is independent of α and nearly independent of Q. Therefore, Eq. (37) suggests that $\eta(\xi)$ has similar features as $f(\xi)$. Eq. (36) shows that in calm synoptic conditions over a gentle slope, θ_{*0} depends on thermal and dynamic processes through parameters $h, \beta_{\rm T}$, and α, with θ_{*0} being proportional to $h \sin\alpha$. The value of h, based on Eq. (18), depends not only on Q and Q_1, but also on h_2 and $\beta_{\rm T}$. An intercomparison of Eqs. (36) and (9) shows that the effect of the slope steepness is stronger on θ_{*0} than on u_{*0}. u_{*0}, and is dependent on the total heating in the PBL for the day, but independent of $\beta_{\rm T}$; however θ_{*0} is dependent on the total heating for the day, the total cooling from the previous night, and the depth of the nearly neutral layer remaining from the previous day's PBL. θ_{*0} is proportional to $\beta_{\rm T}^{1/2}$.

5. Conclusions

New parameterizations for turbulent quantities over gently sloping terrain including the friction velocity, temperature scale and the up-slope velocity profile, have been theoretically investigated under steady-state and synoptically calm conditions.

The advantage of the current study is that the friction velocity, temperature scale and the thermally forced up-slope velocity profile can be estimated using routinely measured potential temperature, which is much simpler and much more practical than the schemes proposed by Gutman and Melgarejo (1981) and Hunt et al. (2003) as described in the introduction. The formulations derived by Gutman and Melgarejo (1981) are very complicated because the friction velocity (and temperature scale) is an implicit function of the friction velocity and temperature scale. The friction velocity derived by Hunt et al. (2003) is proportional to the convective velocity but the convective velocity is a function of the product of the friction velocity and the temperature scale. The disadvantage with respect to these formulations is that the parameterized turbulent variables are difficult to use.

The major conclusions are as follows:

(1) The friction velocity u_{*0} is found to be proportional to the product of the square root of the total accumulated heating in the boundary layer (Q) and the sinusoidal function of the slope angle ($\sin\alpha$).

(2) The temperature scale is proportional to the production of the vertical gradient of the potential temperature in the free atmosphere ($\beta_{\rm T}$), the PBL depth (h) and $\sin\alpha$. This indicates that the temperature scale is affected by not only the accumulated heating rate Q but also the total cooling during the previous night, the depth of the nearly neutral layer remaining from the previous day's PBL, and $\beta_{\rm T}$. The impact of the slope angle on the temperature scale is stronger than that on the friction velocity.

(3) The friction velocity is independent of $\beta_{\rm T}$, but the temperature scale however, is proportional to $\beta_{\rm T}^{1/2}$.

(4) The surface momentum flux is proportional to $Q\sin\alpha$. The surface sensible heat flux is proportional to $hQ^{1/2}\beta_{\rm T}\sin^{3/2}\alpha$.

(5) The upslope wind profile in a non-dimensional coordinate ξ, $u(\xi)$ is directly proportional to $(Q\sin\alpha)^{1/2}$ and therefore, directly proportional to the friction velocity.,

Acknowledgements. This study was supported by the National Natural Science Foundation of China (Grant No. 40233032), Ministry of Science and Technology (Grant No. 2006BAB18B03 and Grant No. 2006BAB18B05) and Office of Naval Research (Grant No. N0001409WR20177). The National Center for Atmospheric Research is sponsored by the National Science Foundation of USA.

REFERENCES

Abbs, D. J., and R. A. Pielke, 1986: Thermally forced surface flow and convergence patters over northeast Colorado. *Mon. Wea. Rev.*, **14**, 2281–2296.

André, J. C., and L. Mahrt, 1982: The nocturnal surface inversion and influence of clear-air radiative cooling. *J. Atmos. Sci.*, **39**, 864–878.

Banta, B., and W. R. Cotton, 1981: An analysis of the structure of local wind systems in a broad mountain basin. *J. Appl. Meteor.*, **20**, 1255–1266.

Bourras, D., 2006: Comparison of five satellite-derived latent heat flux products to Moored Buoy Data. *J. Climate*, **15**, 6291–6313.

Chen, R. R., N. S. Berman, D. L. Boyer, and H. J. S. Fernando, 1996: Physical model of the diurnal heating in the vicinity of a two-dimensional ridge. *J. Atmos. Sci.*, **53**, 62–85.

Chou, S.-H., E. Nelkin, J. Ardizzone, R. M. Atlas, and C.-L. Shie, 2003: Surface turbulent heat and momentum fluxes over global oceans based on the Goddard satellite retrievals, Version 2 (GSSTF2). *J. Climate*, **16**, 3256–3273.

Clark, R. H., R. R. Brook, D. G. Reid, and A. J. Troup, 1971: The Wangara experiment: Boundary layer data. Tech. Paper No. 19, Div. Meteor. Phys., CSIRO, Aspendale, Victoria, Australia, 341pp.

Defant, F., 1951: Local winds. *Compendium of Meteorology*, T. F. Malone, Ed., Amer. Meteor., Soc., 655–672.

Garrat, J. R., and B. F. Ryan, 1989: The structure of the stable stratified internal boundary layer in offshore flow over the sea. *Bound.-Layer Meteor.*, **47**, 17–40.

Gutman, L. N., and J. Q. Melgarejo, 1981: On the laws

of geostrophic drag and heat transfer over a slightly inclined terrain. *J. Atmos. Sci.*, **38**, 1714–1724.

Hunt, J. C. R., H. J. Fernando, and M. Princevac, 2003: Unsteady thermally driven flows on gentle slopes. *J. Atmos. Sci.*, **60**, 2169–2182.

Kao, S. K., 1981: An analytical solution for three-dimensional stationary flows in the atmospheric boundary layer over terrain. *J. Appl. Meteor.*, **20**, 386–390.

Lettau, H. H., and B. Davidson, 1957: *Exploring the Atmosphere's First Mile.* Vol. II, Pergamon Press, 557pp.

McNider, R. T., and R. A. Pielke, 1981: Diurnal boundary layer development over sloping terrain. *J. Atmos. Sci.*, **38**, 2198–2212.

O'Brien, James J., 1970: A note on the vertical structure of the eddy exchange coefficient in the planetary boundary layer. *J. Atmos. Sci.*, **27**, 1213–1215.

Pielke, R. A., 1984: *Mesoscale Meteorological Modeling.* Academic Press, New York, 612pp.

Pielke, R. A., and M. Segal, 1986: Mesoscale circulations forced by differential terrain heating. *Mesoscale Meteorology and Forecasting*, P. S. Ray, Ed., Amer. Meteor. Soc., Boston, Mass, 516–548.

Pielke, R. A., H. A. Panofsky, and M. Segal, 1983: A suggested refinement for O'Brien's convective boundary layer eddy exchange coefficient formulation. *Bound.-Layer Meteor.*, **26**, 191–195.

Princevac, M., and A. Venkatram, 2007: Estimating micrometeorological inputs for modeling dispersion in urban areas during stable conditions. *Atmos. Environ.*, **41**, 5345–5356.

Stephan, F. J. De Wekker, D. G. Steyn, M. W. Rotach, J. D. Fast, and S. Zhong, 2002: Observations and numerical modeling of the daytime boundary layer structure in the Rivera valley, Switzerland. *10th Conference on Mountain Meteorology and MAP Meeting*, 13–21, Park City, UT.

Stevens, B., 2000: Quasi-steady analysis of a PBL model with an eddy-diffusivity profile and nonlocal fluxes. *Mon. Wea. Rev.*, **128**, 824–836.

Stewart, J. Q., C. D. Whiteman, W. J. Steenburgh, and X. Bian, 2001: A climatological study of thermally driven wind systems of US intermountain west. *Bull. Amer. Meteor. Soc.*, **83**, 699–708.

Troen, I., and L. Mahrt, 1986: A simple model of the atmospheric boundary layer; sensitivity to surface evaporation. *Bound.-Layer Meteor.*, **37**, 129–148.

Venkatram, A., and M. Princevac, 2008: Using measurements in urban areas to estimate turbulent velocities for modeling dispersion. *Atmos. Environ.*, **42**, 3833–3841.

Whiteman, D. W., 1982: Breakup of temperature inversion in deep mountain valleys Part I: Observations. *J. Appl. Meteor.*, **21**, 270–289.

Yasuda, N., J. Kondo, and T. Sato, 1986: Drainage flow observed in a V-shape valley. *J. Meteor. Soc. Japan*, **64**, 283–301.

Ye, Z. J., M. Segal, and R. A. Pielke, 1987: Effects of atmospheric thermal stability and slope steepness on the development of daytime thermally induced upslope flow. *J. Atmos. Sci.*, **44**, 3341–3354.

Zhong, S., C. D. Whiteman, and X. Bian, 2004: Diurnal evolution of three-dimensional wind and temperature structure in California's central valley. *J. Appl. Meteor.*, **43**, 1679–1699.